

Fourier transform emission spectroscopy and *ab initio* calculations on OsN

R. S. Ram

Department of Chemistry, University of Arizona, Tucson, Arizona 85721

J. Liévin

Université Libre de Bruxelles, Laboratoire de Chimie Physique Moléculaire, CP 160/09 Av. F. D. Roosevelt 50, Bruxelles, Belgium

P. F. Bernath

Department of Chemistry, University of Arizona, Tucson, Arizona 85721 and Department of Chemistry, University of Waterloo, Waterloo, Ontario N2L 3G1, Canada

(Received 3 May 1999; accepted 28 May 1999)

The emission spectrum of OsN has been recorded in the 3000–13 000 cm^{-1} region using a Fourier transform spectrometer. OsN molecules were excited in an osmium hollow cathode lamp operated with neon gas and a trace of nitrogen. Six bands observed in the 8000–12 200 cm^{-1} region have been classified into three transitions, $a^4\Pi_{5/2}-X^2\Delta_{5/2}$, $b^4\Phi_{7/2}-X^2\Delta_{5/2}$, and $b^4\Phi_{5/2}-X^2\Delta_{5/2}$ with the 0–0 band origins near 8381.7, 11 147.9, and 12 127.2 cm^{-1} , respectively. A rotational analysis of these bands provides the following equilibrium constants for the ground electronic state: $\omega_e = 1147.9492(77) \text{ cm}^{-1}$, $\omega_e x_e = 5.4603(36) \text{ cm}^{-1}$, $B_e = 0.493\,381(55) \text{ cm}^{-1}$, $\alpha_e = 0.002\,753(38) \text{ cm}^{-1}$, and $r_e = 1.618\,023(91) \text{ \AA}$. *Ab initio* calculations have been performed on OsN and the spectroscopic properties of the low-lying electronic states have been calculated. Our assignments are supported by these calculations. The ground state of OsN has been identified as a $^2\Delta_i$ state consistent with the observations for the isoelectronic IrC molecule [Jansson *et al.*, *Chem. Phys. Lett.* **4**, 188 (1969); *J. Mol. Spectrosc.* **36**, 248 (1970)]. The $1\sigma^2 2\sigma^2 1\pi^4 1\delta^3 3\sigma^2$ electron configuration has been proposed for the ground state and the configurations for the other low-lying electronic states have also been discussed. This work represents the first experimental or theoretical investigation of the electronic spectra of OsN. © 1999 American Institute of Physics. [S0021-9606(99)00932-0]

I. INTRODUCTION

The transition metal-containing molecules are of importance as catalysts in organic and organometallic chemistry.^{1–4} Spectroscopic studies of these molecules provide insight into chemical bonding in simple metal-containing systems.⁵ Transition metal-containing species are also of astrophysical importance. Several of transition metal atoms and the corresponding diatomic oxides and hydrides have been identified in the atmospheres of cool *M*- and *S*-type stars.^{6–10} Although the search for transition metal nitrides in stellar atmospheres has not been successful so far, such observations might provide the information on the abundance of nitrogen in the atmospheres of cool stars. Precise spectroscopic data are necessary for a meaningful search for transition metal nitrides in complex stellar spectra.

In recent years a number of transition metal nitride molecules have been observed in the gas phase and their electronic spectra have been characterized at high resolution. For the *5d* transition metal family, in particular, high resolution spectroscopic data are now available for HfN,¹¹ WN,¹² ReN,^{13,14} IrN (Refs. 15,16), and PtN (Refs. 17,18). In the present paper we report the first observation of another *5d* transition metal nitride, OsN, using the technique of Fourier transform emission spectroscopy.

Among Os-containing diatomic molecules only limited spectroscopic data are available for OsO, obtained by optical

emission spectroscopy.¹⁹ Although no previous theoretical or experimental data are available on OsN to help us in the interpretation of the observed spectra, our assignments are consistent with the previous experimental^{15,20,21} and theoretical²² work on the isoelectronic IrC molecule. The OsN bands observed in the 8000–12 200 cm^{-1} interval have been assigned to three transitions, $a^4\Pi_{5/2}-X^2\Delta_{5/2}$, $b^4\Phi_{7/2}-X^2\Delta_{5/2}$, and $b^4\Phi_{5/2}-X^2\Delta_{5/2}$. The lowest $X^2\Delta_{5/2}$ state has been assigned as the ground state of OsN consistent with the observations for the isoelectronic IrC molecule,^{15,20,21} as well as our *ab initio* calculations.

II. EXPERIMENT

The spectra of OsN were observed in an osmium hollow cathode lamp which was prepared by pressing a mixture of Os and Cu powders (ratio 1:3) in a 10 mm hole in a copper block. The block was then bored through to provide approximately 1 mm thick layer of the mixture on the inside wall of the cathode. The lamp was operated with a current at 550 mA and 250 V by flowing a mixture of 2.3 Torr of Ne and about 10 mTorr of N_2 through the lamp. The emission from the lamp was observed with the 1 m Fourier transform spectrometer associated with the McMath–Pierce solar telescope of the National Solar Observatory. The spectrometer was equipped with a CaF_2 beam splitter.

The spectra from 3000 to 13 000 cm^{-1} were recorded using InSb detectors and a red pass (Schott 780) filters with 40 scans coadded in about 5 h of integration. The spectrometer resolution was set at 0.03 cm^{-1} . In addition to the OsN bands, the observed spectra also contained Os and Ne atomic lines as well as much stronger N_2 molecular lines. Although the OsN bands are much weaker in intensity than the N_2 bands, OsN molecular lines were easily identified due to their smaller line spacing in a branch. In order to ascertain the carrier of these bands, the flow of N_2 was replaced with ~ 150 mTorr flow of O_2 in a subsequent experiment. The newly observed bands disappeared completely and again reappeared when N_2 replaced O_2 . This experimental evidence confirmed that the new bands were indeed due to OsN.

The line positions were extracted from the observed spectra using a data reduction program called PC-DECOMP developed by Braut. The peak positions were determined by fitting a Voigt line shape function to each spectral feature. The branches in the different subbands were sorted using a color Loomis–Wood program running on a PC computer. The spectra were calibrated using the measurements of Ne atomic lines made by Palmer and Engleman.²³ The absolute accuracy of the wavenumber scale is expected to be of the order of ± 0.003 cm^{-1} . The OsN lines in the stronger bands appear with a maximum signal to noise ratio of about ten and have a typical line width of about 0.04 cm^{-1} . The precision of measurements of strong and unblended OsN lines is expected to be better than ± 0.003 cm^{-1} . However, the 1–1 band of the $a^4\Pi_{5/2}-X^2\Delta_{5/2}$ transition has about 50% of the intensity of the 0–0 band and the $b^4\Phi_{5/2}-X^2\Delta_{5/2}$ lines are frequently overlapped by N_2 lines. The precision of measurements for the weaker and overlapped lines is limited to ± 0.005 cm^{-1} .

III. AB INITIO CALCULATIONS

Large scale *ab initio* calculations have been performed on the low-lying doublet, quartet, and sextet states of OsN in order to predict the electronic structure of this new molecule. A total of thirteen electronic states have been investigated, corresponding to the low-lying states in each spatial and spin symmetry. The calculations have been performed with the internally-contracted multireference configuration interaction method (CMRCI)²⁴ using the electron core potentials and basis sets developed in the theoretical chemistry group of Stuttgart.^{25,26} Referring to our previous work on RuN (Ref. 27) and on IrN (Ref. 28), in which the same computational approach was adopted, we expect reliable predictions of the spectroscopic properties: typically within 0.02 Å for the equilibrium internuclear distances, within 50 cm^{-1} for harmonic vibrational frequencies, and within 2000 cm^{-1} for the term energies.

The potential energy surfaces have been calculated at ten geometries ranging from 1.5 to 2.0 Å, and at each of these points the following two-step procedure has been applied. All valence orbitals (four σ , two π , and one δ orbitals arising from the 5*d* and 6*s* orbitals of osmium and from the 2*s* and 2*p* orbitals of nitrogen) were first optimized at the CASSCF level²⁹ (complete active space self-consistent field), using a state averaging procedure within each different spin system.

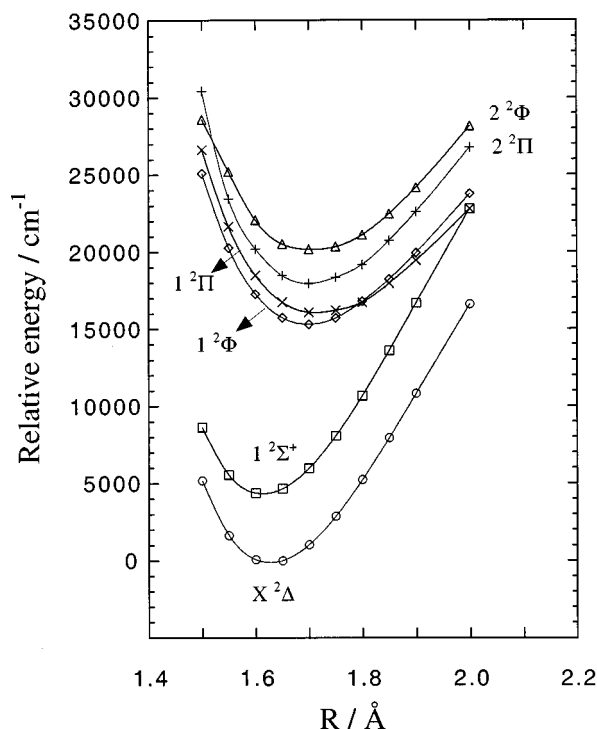


FIG. 1. The low-lying doublet potential energy curves of OsN from CMRCI calculations.

These orbitals were then used in a CMRCI calculation, in which all valence electrons were correlated. The CMRCI energies were corrected for Davidson's contribution³⁰ for unlinked four-particle clusters. Quasirelativistic pseudopotentials have been used to represent the 60 core electrons of the osmium atom²⁵ and the two 1*s* electrons of nitrogen.²⁶ The corresponding valence double zeta basis sets^{25,26} were augmented by a single *f* Gaussian orbital on Os and a single *d* polarization function on N, both with an exponent of 0.8. The size of the corresponding CASSCF (CMRCI) wavefunctions are ranging between 480 and 3460 (146 000 and 460 000) configuration state functions in C_{2v} symmetry, depending on the space and spin symmetries.

All calculations were performed with the MOLPRO program package³¹ running on the Cray J916 computer at the ULB/VUB computer center.

IV. ELECTRONIC STRUCTURE OF OsN AND AB INITIO RESULTS

The potential energy curves calculated at the CMRCI level of theory are shown in Figs. 1, 2, and 3, for the doublet, quartet, and sextet spin manifolds, respectively. The energy scale used in these figures is relative to the minimum energy of the ground electronic state. The relative energies between the different spin systems is better illustrated in Fig. 4. Some higher energy states, indicated in dotted lines on this figure, involve stronger configuration mixing (see below) that would justify further larger scale calculations. The corresponding term energies, reported on Fig. 4, are thus expected to be less accurate (within about 4000 cm^{-1}) than those of the other states.

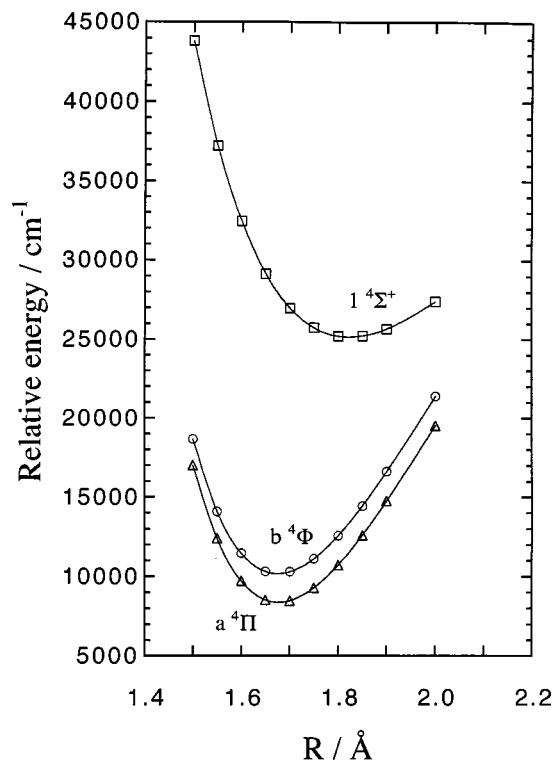


FIG. 2. The low-lying quartet potential energy curves of OsN from CMRCI calculations.

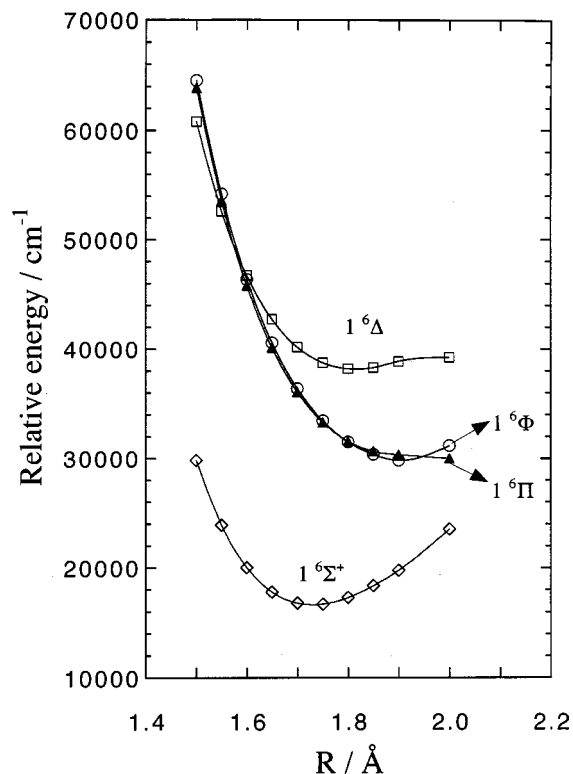


FIG. 3. The low-lying sextet potential energy curves of OsN from CMRCI calculations.

The correlation diagram drawn in Fig. 5 allows an interpretation of the electronic structure of OsN, as predicted by our CMRCI calculations. This figure correlates the molecular orbitals of OsN to those of the osmium and nitrogen atoms in their ground state. This diagram has been obtained from size-consistent full-valence CASSCF calculations performed on the different species: OsN, Os(5D) and N(4S). The OsN orbitals were obtained from a state-averaged CASSCF calculation performed, at an internuclear distance of 1.65 Å, on the doublet states correlating to the ground dissociation channel Os(5D) and N(4S). The dotted lines connecting the orbitals of OsN to those of the atomic products give a qualitative information on the linear combination of atomic orbital (LCAO) content of the molecular orbitals provided by the analysis of the CASSCF wavefunctions. It is interesting to compare this diagram with those obtained for other transition metal nitrides, like RuN (Ref. 27) and IrN (Ref. 28), investigated with the same computational approach. This comparison may be worthwhile, since RuN is a $4d$ transition metal compound isovalent to OsN, and IrN has a single electron more than OsN. It is found that the bonding and antibonding mixtures of atomic orbitals are quite similar in the three systems. What differs, however, is the energy difference between the 1δ and 3σ molecular orbitals (0.156, 0.089, and 0.041 a.u. for RuN, IrN, and OsN, respectively), which can be related to the energy gap between the nd and $(n+1)s$ atomic orbitals of the transition metal ($n=4$ for Ru and $n=5$ for Os and Ir). This last difference is -0.115 , -0.137 , and $+0.066$ a.u. for Ru, Ir, and Os, respectively, showing an inversion of the s and d orbitals along this series. The consequence of this is to enhance the $6s(\text{Os})-2p\sigma(\text{N})$

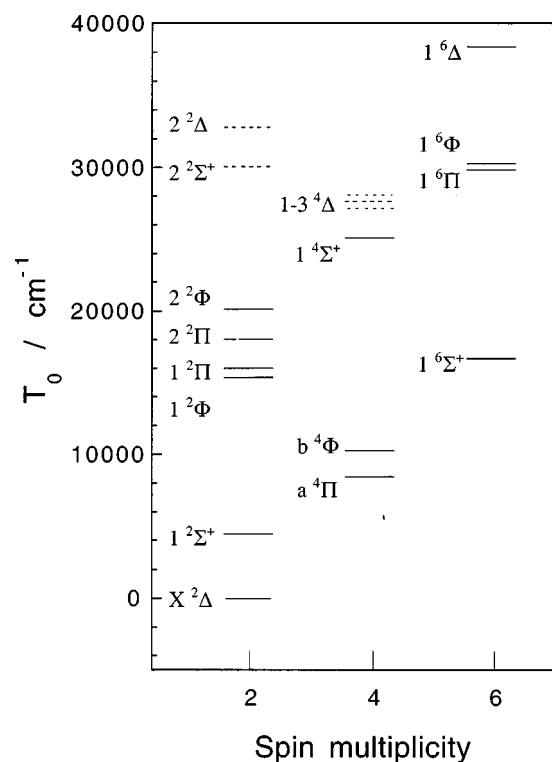


FIG. 4. Relative energies within the different spin systems of OsN from CMRCI calculations.

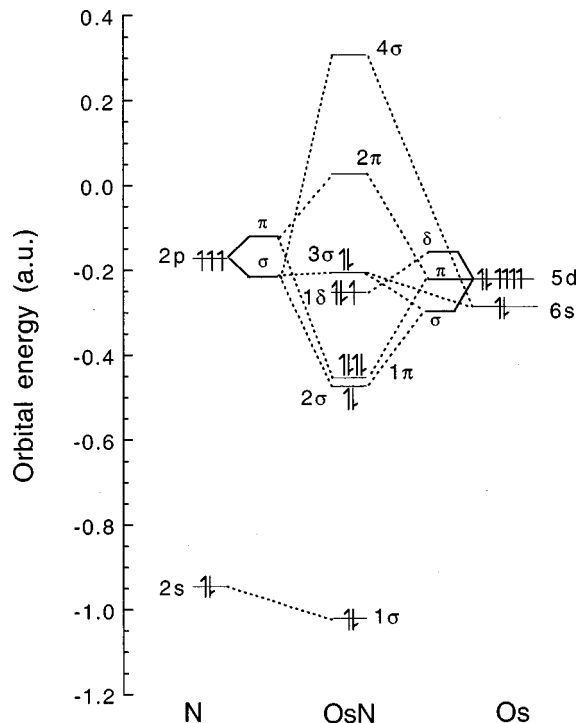


FIG. 5. The molecular orbital correlation diagram for OsN from CASSCF calculations.

bonding character of the 3σ orbital and consequently the corresponding antibonding character of the 4σ orbital. This explains why RuN and OsN have different ground electronic configurations ($3\sigma^1 1\delta^4$ and $3\sigma^2 1\delta^3$, respectively) and why the 4σ orbital does not contribute to the excited states of OsN (see Tables I and II).

In agreement with the electron orbital filling in Fig. 5, the ground state ($X^2\Delta$) of OsN arises from configuration $1\sigma^2 2\sigma^2 1\pi^4 1\delta^3 3\sigma^2$. This is confirmed by the analysis of the corresponding CMRCI wavefunction, to which this configuration contributes 78%.

TABLE I. Electronic configurations describing the low-lying electronic states of OsN (see Table II).

Label	Configuration	Electron promotion ^a
(A)	$1\sigma^2 2\sigma^2 1\pi^4 1\delta^3 3\sigma^2$	
(B)	$1\sigma^2 2\sigma^2 1\pi^4 1\delta^4 3\sigma^1$	$3\sigma \rightarrow 1\delta$
(C)	$1\sigma^2 2\sigma^2 1\pi^4 1\delta^2 3\sigma^1 2\pi^2$	$1\delta 3\sigma \rightarrow 2\pi^2$
(D)	$1\sigma^2 2\sigma^2 1\pi^3 1\delta^3 3\sigma^2 2\pi^1$	$1\pi \rightarrow 2\pi$
(E)	$1\sigma^2 2\sigma^1 1\pi^4 1\delta^3 3\sigma^1 2\pi^2$	$2\sigma 3\sigma \rightarrow 2\pi^2$
(F)	$1\sigma^2 2\sigma^2 1\pi^3 1\delta^3 3\sigma^1 2\pi^2$	$1\pi 3\sigma \rightarrow 2\pi^2$
(G)	$1\sigma^2 2\sigma^2 1\pi^4 1\delta^3 3\sigma^1 2\pi^1$	$3\sigma \rightarrow 2\pi$
(H)	$1\sigma^2 2\sigma^2 1\pi^4 1\delta^2 3\sigma^2 2\pi^1$	$1\delta \rightarrow 2\pi$
(I)	$1\sigma^2 2\sigma^2 1\pi^3 1\delta^4 3\sigma^1 2\pi^1$	$1\pi 3\sigma \rightarrow 1\delta 2\pi$
(J)	$1\sigma^2 2\sigma^2 1\pi^3 1\delta^3 3\sigma^2 2\pi^2$	$1\pi 1\delta \rightarrow 2\pi^2$
(K)	$1\sigma^2 2\sigma^2 1\pi^2 1\delta^3 3\sigma^2 2\pi^2$	$1\pi^2 \rightarrow 2\pi^2$
(L)	$1\sigma^2 2\sigma^2 1\pi^2 1\delta^4 3\sigma^1 2\pi^2$	$1\pi^2 3\sigma \rightarrow 1\delta 2\pi^2$
(M)	$1\sigma^2 2\sigma^2 1\pi^3 1\delta^2 3\sigma^1 2\pi^3$	$1\pi 1\delta^2 \rightarrow 2\pi^3$
(N)	$1\sigma^2 2\sigma^2 1\pi^2 1\delta^3 3\sigma^1 2\pi^3$	$1\pi^2 3\sigma \rightarrow 2\pi^3$
(O)	$1\sigma^2 2\sigma^2 1\pi^4 1\delta^1 3\sigma^2 2\pi^2$	$1\delta^2 \rightarrow 2\pi^2$
(P)	$1\sigma^2 2\sigma^2 1\pi^4 1\delta^3 3\sigma^1 4\sigma^1$	$3\sigma \rightarrow 4\sigma$

^aElectron promotions are defined with respect to the ground electronic configuration (A).

TABLE II. Analysis of the CMRCI wave functions of OsN in terms of electronic configurations.^{a,b}

Electronic state	Weight
$X^2\Delta$	78% (A) + 6% (K)
$1^2\Sigma^+$	77% (B) + 4% (L)
$1^2\Phi$	75% (G) + 3% (H) + 3% (N)
$1^2\Pi$	40% (G) + 31% (H) + 3% (N)
$2^2\Pi$	34% (G) + 41% (H) + 3% (J)
$2^2\Phi$	47% (G) + 31% (H)
$a^4\Pi$	66% (G) + 14% (H) + 3% (N)
$b^4\Phi$	80% (G) + 3% (N)
$1^4\Sigma^+$	67% (C) + 9% (I) + 6% (M)
$1^6\Sigma^+$	79% (C) + 3% (M)
$1^6\Phi$	85% (E)
$1^6\Pi$	64% (F) + 17% (J)
$1^6\Delta$	85% (E)
$2^2\Sigma^+$	49% (C) + 17% (I) + 7% (M)
$2^2\Delta$	69% (D) + 3% (I) + 3% (O)
$1,2,3^4\Delta$	Strong mixing of (C), (D), and (O)

^aWeights (in percent) are obtained from the square of the corresponding configuration interaction coefficients; weights lower than 3% are not reported.

^bSee Table I for the definition of the configuration labeling.

The electronic structure of OsN below $40\,000\text{ cm}^{-1}$ (see Tables I to III) can be described in terms of the 16 configurations listed in Table I. These configurations, labeled from (A) to (P), have a weight larger than 3% in the corresponding CMRCI wavefunctions. The configuration weights are given by the square of the corresponding CI coefficients, calculated close to the equilibrium geometry of the considered states. Also given in Table I for each excited configuration is the electron promotion with respect to the ground configuration (A). Table II provides an analysis of the CMRCI wavefunctions of all the states calculated in this work (see Figs. 1 to 4) in terms of configurations (A) to (P) given in Table I. One

TABLE III. Spectroscopic properties of the low-lying electronic states of OsN from CMRCI calculations. Experimental values from this work are given in parentheses.

Spin multiplicity	State	T_0 (cm ⁻¹)	R_e (Å)	ω_e (cm ⁻¹)
2	$X^2\Delta$	0	1.627	1146
			(1.618 02) ^a	(1147.95) ^a
	$1^2\Sigma^+$	4464.8	1.614	1169
	$1^2\Phi$	15 336.8	1.697	940
	$1^2\Pi$	16 000.0	1.720	841
	$2^2\Pi$	18 016.4	1.703	843
	$2^2\Phi$	20 116.0	1.704	933
4	$a^4\Pi$	8445	1.677	1003
		(8381.75) ^b	(1.655 22) ^b	(1045.61) ^b
	$b^4\Phi$	10245	1.675	1004
		(11 147.92,		
		12 127.19) ^c	1.675	1004
	$1^4\Sigma^+$	25 064	1.822	712
6	$1^6\Sigma^+$	16 650	1.730	884
	$1^6\Phi$	29 813	1.912	...

^aFrom $X^2\Delta_{5/2}$ (from this work).

^bFrom $a^4\Pi_{5/2}$ (from this work).

^cFrom $b^4\Phi_{7/2}$ and $b^4\Phi_{5/2}$, respectively (from this work).

sees that some states exhibit strong configuration mixing, namely (G) and (H) mixing for the $1^2\Pi$, $2^2\Pi$, $2^2\Phi$ and $a^4\Pi$ states, and (F) and (J) mixing for the $1^6\Pi$ state. In both cases the configurations that are involved, differing by a single $3\sigma \rightarrow 1\delta$ excitation, are expected to be close in energy owing to the small $3\sigma-1\delta$ energy gap. Some higher energy states, like those drawn in dotted lines in Fig. 4 ($2^2\Sigma^+$ and the 1, 2, and 3 $^4\Delta$ states) exhibit multiple avoided crossings within the range of distances of 1.5 to 2.0 Å. This is due to the existence of close-lying configurations in the corresponding energy region. The resulting potential energy curves have not been reported in Figs. 1 and 2, because such configuration mixing would have needed larger CASSCF active spaces than considered here.

Most other states are described by a single leading configuration characterized by a weight between 75% and 85%. The weight of the secondary configurations are quite small and the remaining contributions are distributed over a large number of configurations. Notice that, as already observed in RuN (Ref. 27) and IrN (Ref. 28), it is important to take these correlation effects into account to make the calculated spectroscopic properties converge to a reasonable accuracy. These properties, i.e., the equilibrium internuclear distance R_e , the harmonic frequencies at equilibrium ω_e , and the term energies T_0 , corrected for the zero-point energy contribution calculated within the harmonic approximation are reported in Table III, where they are also compared to the available experimental values. The agreement is of the same order-of-magnitude as in the other systems previously investigated with the same computational approach,^{27,28} with discrepancies of about 1% for R_e (less than 0.02 Å) and less than 4% (40 cm^{-1}) for ω_e . The good agreement for the T_0 values (63 cm^{-1} for the $a^4\Pi$ state and 1394 cm^{-1} for the $b^4\Phi$ state with respect to the average of the experimental values for the $\Omega=7/2$ and $5/2$ spin components of this state) confirms the assignment of the observed transition, as schematized in Fig. 6. Note that no other candidates other than the $a^4\Pi$ and $b^4\Phi$ states are predicted by our *ab initio* calculations, as clearly shown in Fig. 4, in the energy window between 4000 and 15000 cm^{-1} .

V. OBSERVATION AND ANALYSIS

The newly observed bands of OsN are located in the 8000–12200 cm^{-1} region. All of these bands are degraded towards lower wavenumbers and appear with moderate intensity. Although the first lines were not clearly identified in any of the bands the Ω -assignments were made using the relative intensities of the branches and by comparison with IrC. The observed bands have been classified into three transitions, $a^4\Pi_{5/2}-X^2\Delta_{5/2}$, $b^4\Phi_{7/2}-X^2\Delta_{5/2}$, and $b^4\Phi_{5/2}-X^2\Delta_{5/2}$ on the basis of our *ab initio* calculations (see previous section) and those for IrC. A schematic energy level diagram of the observed transitions of OsN is provided in Fig. 6 where the electronic states predicted from *ab initio* calculations are also provided for comparison. All three transitions involve a common lower state.

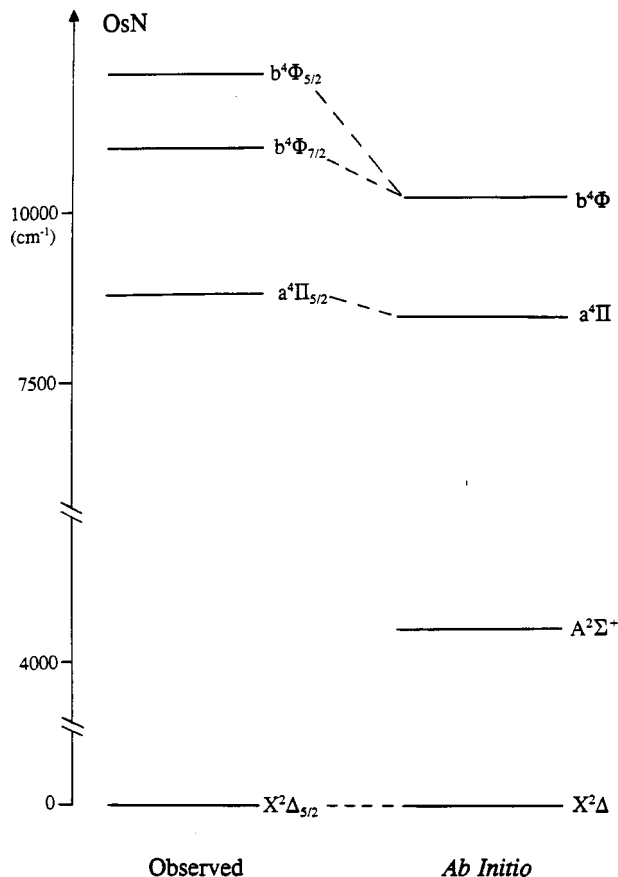


FIG. 6. A schematic energy level diagram of the observed transitions of OsN.

A. The $a^4\Pi_{5/2}-X^2\Delta_{5/2}$ system

The 0–0 band of this transition is located near 8381.75 cm^{-1} . This band is the strongest of all bands assigned to this transition and appears with a maximum signal-to-noise ratio of 10:1. The structure consists of only two branches, one *R* and one *P*, both appearing with similar intensity. The lines up to $J=45.5$ were identified in the *R* and *P* branches of this transition. The 1–1 band of this transition located near 8290 cm^{-1} is much weaker in intensity than the 0–0 band and lines up to $J=28.5$ and 37.5 were identified in the *R* and *P* branches of this band. The 2–2 and other higher vibrational bands of this sequence could not be identified. On the lower wavenumber side, two bands located near 7245 and 7165 cm^{-1} have been identified as the 0–1 and 1–2 bands of the $a^4\Pi_{5/2}-X^2\Delta_{5/2}$ transition.

The Os atom has four principal isotopes ^{192}Os , ^{190}Os , ^{189}Os , and ^{188}Os in the approximate proportion of 3:2:1:1. The lines due to the minor isotopomer ^{190}OsN were also identified, at least in the 0–1 and 1–2 bands, but the molecular constants for ^{190}OsN were not extracted because of their very weak intensity. All four bands of this transition were rotationally analyzed. The analysis of the bands belonging to the $a^4\Pi_{5/2}-X^2\Delta_{5/2}$ transition provide a complete set of equilibrium constants for the ground state of OsN.

B. The $b^4\Phi_{7/2}-X^2\Delta_{5/2}$ and $b^4\Phi_{5/2}-X^2\Delta_{5/2}$ systems

Two further high wavenumber bands with the band origins near 11147.92 cm^{-1} and 12127.17 cm^{-1} have been

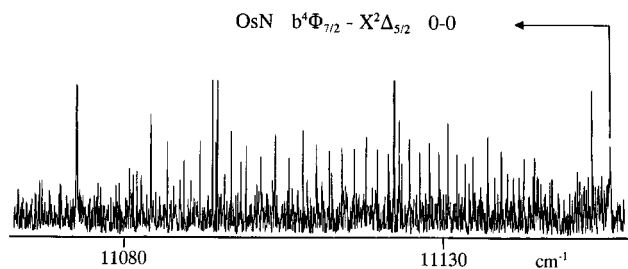


FIG. 7. A portion of the 0–0 band of the $b^4\Phi_{7/2}-X^2\Delta_{5/2}$ transition of OsN.

assigned as the 0–0 bands of the $b^4\Phi_{7/2}-X^2\Delta_{5/2}$ and $b^4\Phi_{5/2}-X^2\Delta_{5/2}$ transitions, respectively. The $b^4\Phi_{7/2}-X^2\Delta_{5/2}$ transition consists of three branches, one R , one P , and one Q , with the Q branch being the strongest and R and P branches appearing with similar intensity. The $b^4\Phi_{5/2}-X^2\Delta_{5/2}$ 0–0 band consists of only one R and one P branch. No Ω -doubling is observed in any of these bands and no perturbations have been detected over the range of observed J values. No other $\Delta v \neq 0$ bands belonging to the $b^4\Phi_{7/2}-X^2\Delta_{5/2}$ and $b^4\Phi_{5/2}-X^2\Delta_{5/2}$ transitions were identified in our spectra and, therefore, the vibrational intervals in the $b^4\Phi_{7/2}$ and $b^4\Phi_{5/2}$ states remain still to be determined. A part of the spectrum of the $b^4\Phi_{7/2}-X^2\Delta_{5/2}$ 0–0 band is provided in Fig. 7. Unfortunately the first lines were again not identified in these bands because of their weak intensity and overlapping from the head-forming R branch. The excited states of these two transitions have been assigned as the $\Omega = 7/2$ and $\Omega = 5/2$ states, respectively, on the basis of the number of branches and lack of any observable Ω -doubling. These two states have in turn been assigned as the $^4\Phi_{7/2}$ and $^4\Phi_{5/2}$ states by comparison with our *ab initio* results.

For the rotational analysis of these bands, the blended and weaker lines were given lower weights depending on their signal-to-noise ratio and extent of blending. The observed line positions in these transitions are available from EPAPS³² or from the authors upon request. Since the observed states are spin-components of case (c) states which probably have very large spin-orbit splittings, the molecular constants for each observed state were determined by fitting the observed wavenumbers to the customary empirical energy level expression for the ground and excited states given as follows:

$$F(J) = T_v + B_v J(J+1) - D_v [J(J+1)]^2.$$

Because of the lack of observable Ω -splitting, no

Ω -doubling parameters were included in the energy level expression. The rotational constants obtained from the final fit are provided in Table IV.

VI. DISCUSSION

In our recent investigation of several transition metal nitrides we have noted that the electronic structure of some nitrides particularly in the group VIII family of transition metals are very similar to that of the isoelectronic diatomic carbides molecules. For example, IrN (Refs. 14,15) & PtC (Refs. 32–36) and RuN (Ref. 27) & RhC (Ref. 37) have very similar electronic structure. It has also been noted that a similar correspondence does not exist between the isoelectronic oxides and nitrides. The close similarity of group VIII transition metal nitrides and isoelectronic carbides suggests that the electronic structure of OsN should be very similar to the electronic structure of IrC (Refs. 15,20,21). Since there were no previous theoretical calculations for OsN, the initial analysis proceeded using the results available for the IrC.

A schematic diagram of the low-lying electronic states of IrC is presented in Fig. 8. The ground state of IrC has been assigned as $X^2\Delta_{5/2}$ spin component of a $^2\Delta_i$ state.^{15,20–22} The low-lying $X^2\Delta_{3/2}$ spin component was also detected, but the spin-orbit interval was not determined directly by Jansson and Scullman.²¹ The effective B values for the two spin components implied that the $^2\Delta_{3/2}-^2\Delta_{5/2}$ interval was about 3200 cm^{-1} . Tan *et al.*²² calculated that this interval should be about 6500 cm^{-1} and attempted to reassign Jansson and Scullman's $X^2\Delta_{3/2}$ state as a $^2\Sigma^+$ state. This reassignment is erroneous because Jansson and Scullman saw first lines in a $^2\Delta_{3/2}-X^3\Delta_{3/2}$ transition without Ω -doubling or spin-splitting, thus excluding a $^2\Sigma^+-^2\Sigma^+$ assignment. The $^2\Delta_{3/2}-^2\Delta_{5/2}$ interval, however, could well be close to 6000 cm^{-1} as calculated by Tan *et al.*²² because the use of effective B values to determine this interval is unreliable for heavy molecules such as IrC. Hund's case (c) tendencies in IrC would shift the B_{eff} values away from those expected for an isolated $^2\Delta$ state. The very low-lying $^2\Sigma^+$ state of IrC has not been seen yet but the $a^4\Phi$ state is calculated to lie at 12 500 cm^{-1} (without spin-orbit splitting) moderately close to a 5/2 state at 15 100 cm^{-1} $E_1^2\Delta_{5/2}$ and a 7/2 state at 14 350 cm^{-1} (see Fig. 8). Thus Jansson and Scullman's $D^2\Phi_{7/2}$ state is the $a^4\Phi_{7/2}$ state and $E_1^2\Delta_{5/2}$ is the $a^4\Phi_{5/2}$ state with the $E_2^2\Delta_{3/2}$ shifted 3000 cm^{-1} to higher energy. The $E_2^2\Delta_{3/2}$ state is thus probably the $b^4\Pi_{3/2}$ state with a strong admixture of $B^2\Pi_{3/2}$.

TABLE IV. Spectroscopic constants (in cm^{-1}) for the $X^2\Delta_{5/2}$, $a^4\Pi_{5/2}$, $b^4\Phi_{7/2}$, and $b^4\Phi_{5/2}$ states of OsN.^a

Const.	$X^2\Delta_{5/2}$			$a^4\Pi_{5/2}$		$b^4\Phi_{7/2}$	$b^4\Phi_{5/2}$
	v=0	v=1	v=2	v=0	v=1	v=0	v=0
T_v	0.0	1137.0286(27)	2263.1366(61)	8381.7512(17)	9427.3656(57)	11147.9306(15)	12 127.1851(24)
B_v	0.492 020(15)	0.489 219(16)	0.486 537(25)	0.470 174(15)	0.467 613(24)	0.464 336(15)	0.469 278(19)
$D_v \times 10^7$	3.513(54)	3.517(60)	4.70(13)	3.643(53)	4.67(13)	3.717(52)	4.45(13)
$H_v \times 10^{11}$	-7.35(36)

^aValues in parentheses are one standard deviation in the last digits.

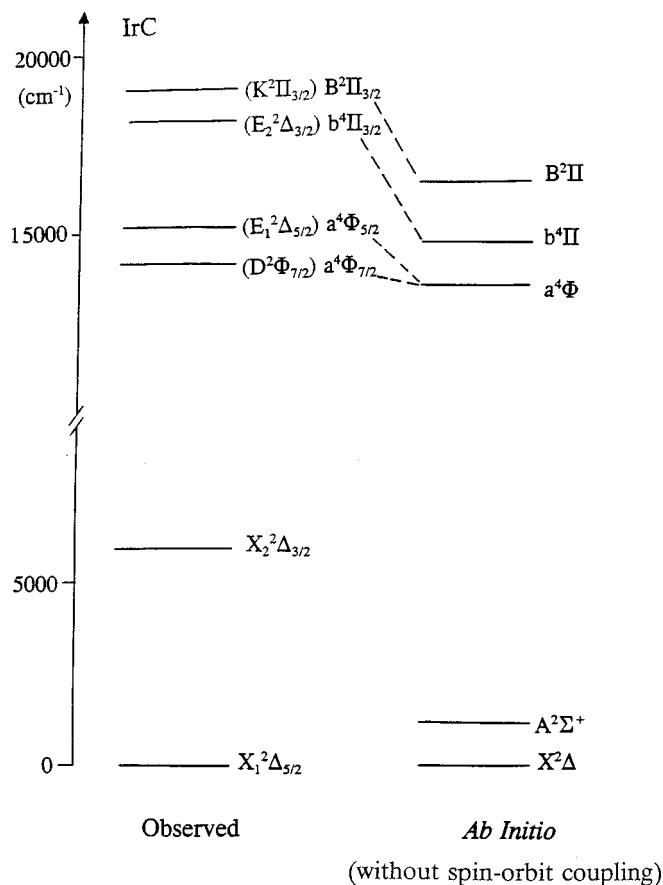


FIG. 8. A schematic energy level diagram of the low-lying electronic states of IrC.

The situation is very similar for OsN with exception that the ordering of the ${}^4\Phi$ and ${}^4\Pi$ states switched (Figs. 4, 6). We find that the $a^4\Pi_{5/2}$ state lies at 8381 cm^{-1} , the $b^4\Phi_{7/2}$ state at $11\,147\text{ cm}^{-1}$, and the $b^4\Phi_{5/2}$ state at $12\,127\text{ cm}^{-1}$.

Os and Ir have $6s^25d^6$ and $6s^25d^7$ as the lowest energy atomic configurations, respectively. The $2s$ orbital of N ($2s^22p^3$) and C ($2s^22p^2$) atoms lie about 3 eV lower than the $2p$ orbitals and do not play a significant role in bonding in OsN and IrC. Since the energy separation between the lowest energy configurations and the excited $6s^15d^7$ and $5d^8$ configurations is very small and the atomic spin-orbit separation for the ground 5D term of the Os atom is quite large, OsN is expected to have a high density of low-lying electronic states, as confirmed by our *ab initio* calculations. By comparing our theoretical results with those of Tan *et al.*²² for IrC one finds that both molecules have a similar electronic structure, at least for the low-lying electronic states and configurations, i.e., that the ground state arises from configuration $1\sigma^22\sigma^21\pi^41\delta^33\sigma^2$ for $X^2\Delta$ state, and that the first excited states arise from the configurations,

$$1\sigma^22\sigma^21\pi^41\delta^43\sigma^1 \rightarrow {}^2\Sigma^+,$$

$$1\sigma^22\sigma^21\pi^41\delta^33\sigma^12\pi^1 \rightarrow {}^2\Pi, {}^2\Phi, {}^4\Pi, {}^4\Phi.$$

This clearly indicates that the observed electronic states $a^4\Pi_{5/2}$, $b^4\Phi_{7/2}$, and $b^4\Phi_{5/2}$ all arise from the electronic configuration $1\sigma^22\sigma^21\pi^41\delta^33\sigma^12\pi^1$. The assignment of $b^4\Phi_{7/2}$ and $b^4\Phi_{5/2}$ states as the spin components of the

TABLE V. Equilibrium constants (in cm^{-1}) for the $X^2\Delta_{5/2}$ and $a^4\Pi_{5/2}$ states of OsN.

Constants ^a	$X^2\Delta_{5/2}$	$a^4\Pi_{5/2}$
ω_e	1147.9492(77)	[1045.6144(59)] ^b
$\omega_e x_e$	5.4603(36)	...
B_e	0.493 381(55)	0.471 455(21)
α_e	0.002 753(38)	0.002 561(28)
$r_e(\text{\AA})$	1.618 023(91)	1.655 220(37)

^aValues in parentheses are one standard deviation in the last digits.

^b $\Delta G(1/2)$ value.

same ${}^4\Phi$ state indicates that this state is inverted. Our *ab initio* calculations predict $a^4\Pi$ and $b^4\Phi$ states at 9989 and $11\,816\text{ cm}^{-1}$, respectively. At present we are unable to predict the regular or inverted nature of the ${}^4\Pi$ or ${}^4\Phi$ states from our *ab initio* calculations.

Our observations indicate that there is no observable doubling in the rotational structure of any of the observed bands indicating that the observed states involve high Ω values consistent with the observations available for the isoelectronic IrC molecule.^{15,20,21} Although the ground state of OsN has been assigned as $X^2\Delta_{5/2}$, the spin-orbit splitting for the ground state could not be determined because no transitions involving the $X^2\Delta_{3/2}$ spin component were seen.

The molecular constants of Table IV have been used in the determination of the equilibrium constants for the $X^2\Delta_{5/2}$ and $a^4\Pi_{5/2}$ states of OsN, which are provided in Table V. The vibrational intervals and equilibrium constants for the $b^4\Phi_{7/2}$ and $b^4\Phi_{5/2}$ states of OsN were not determined due to the absence of $\Delta v = \pm 1$ vibrational bands. However, the observation of bands with $v'' = 0, 1,$ and 2 in the $a^4\Pi_{5/2} - X^2\Delta_{5/2}$ transition allowed equilibrium rotational constants to be determined for the ground state. The equilibrium rotational constants of $0.493\,381(55)$ and $0.471\,455(21)\text{ cm}^{-1}$ provide the equilibrium bond lengths of $1.618\,023(91)$ and $1.655\,220(37)\text{ \AA}$ for the $X^2\Delta_{5/2}$ and $a^4\Pi_{5/2}$ states, respectively. The ground state bond length of $1.618\,023(91)\text{ \AA}$ for OsN can be compared with the ground state bond length of $1.573\,869(10)\text{ \AA}$ for isovalent RuN (Ref. 27) and 1.6830 \AA for the isoelectronic IrC (Ref. 15) molecule. For OsO, a bond length of 1.6847 \AA is obtained using the constants of Balfour and Ram.¹⁹ The ground state vibrational constants of $\omega_e = 1147.9492(77)\text{ cm}^{-1}$, and $\omega_e x_e = 5.4603(36)\text{ cm}^{-1}$ can be compared with the values of $\omega_e = 1122\text{ cm}^{-1}$, and $\omega_e x_e = 6.5\text{ cm}^{-1}$ for isovalent RuN (Ref. 27).

VII. CONCLUSION

We have recorded the emission spectrum of OsN in the $8000\text{--}12\,200\text{ cm}^{-1}$ region using a Fourier transform spectrometer. The six observed bands have been assigned to three transitions, $a^4\Pi_{5/2} - X^2\Delta_{5/2}$, $b^4\Phi_{7/2} - X^2\Delta_{5/2}$, and $b^4\Phi_{5/2} - X^2\Delta_{5/2}$. A rotational analysis of these bands has been carried out and molecular constants have been determined for the ground and excited electronic states. The lowest $X^2\Delta_{5/2}$ state has been assigned as the ground state of OsN, consistent with the observations available for the isoelectronic IrC.^{15,20,21} The ground state of OsN has an equilibrium bond length of $1.618\,023(91)\text{ \AA}$ compared with

1.573 869 Å for RuN (Ref. 27) and 1.6858(1) Å for IrC.¹⁵ The spectroscopic properties of the low-lying electronic states of OsN have been predicted from *ab initio* calculations. Our electronic assignments in general are in excellent agreement with these calculations.

ACKNOWLEDGMENTS

We thank J. Wagner and M. Dulick of the National Solar Observatory for assistance in obtaining the spectra. The National Solar Observatory is operated by the Association of Universities for Research in Astronomy, Inc., under contract with the National Science Foundation. The research described here was supported by funding from the Petroleum Research Fund administered by the American Chemical Society and NASA laboratory astrophysics program. Support was also provided by the Natural Sciences and Engineering Research Council of Canada. J. Liévin thanks the Fonds National de la Recherche Scientifique de Belgique for financial support.

- ¹M. Grunze, in *The Chemical Physics of Solid Surfaces and Heterogeneous Catalysis*, edited by D. A. King and D. P. Woodruff (Elsevier, New York, 1982), Vol. 4, p. 143.
- ²F. A. Cotton and G. Wilkinson, *Advanced Inorganic Chemistry. A Comprehensive Text*, 5th ed. (Wiley, New York, 1988).
- ³M. A. Ciriano, L. A. Oro, and M. T. Camellini, *Organometallics* **15**, 1889 (1996).
- ⁴R. W. Boyle, J. Lautenbach, and W. H. Weinberg, *Ind. Eng. Chem. Res.* **35**, 2986 (1996).
- ⁵C. W. Bauschlicher, Jr., S. P. Walch, and S. R. Langhoff, *Quantum Chemistry: The Challenge of Transition Metals and Coordination Chemistry*, edited by A. Veillard, NATO ASI Ser. C (Reidel, Dordrecht, 1986).
- ⁶D. L. Lambert and R. E. S. Clegg, *Mon. Not. R. Astron. Soc.* **191**, 367 (1980).
- ⁷Y. Yerle, *Astron. Astrophys.* **73**, 346 (1979).
- ⁸B. Lindgren and G. Olofsson, *Astron. Astrophys.* **84**, 300 (1980).
- ⁹O. Engvold, H. Wöhl, and J. W. Brault, *Astron. Astrophys., Suppl. Ser.* **42**, 209 (1980).
- ¹⁰R. S. Ram, P. F. Bernath, and L. Wallace, *Astrophys. J., Suppl. Ser.* **107**, 443 (1996).
- ¹¹R. S. Ram and P. F. Bernath, *J. Mol. Spectrosc.* **184**, 401 (1997).

- ¹²R. S. Ram and P. F. Bernath, *J. Opt. Soc. Am. B* **11B**, 225 (1994).
- ¹³R. S. Ram, P. F. Bernath, W. J. Balfour, J. Cao, C. X. W. Qian, and S. J. Rixon, *J. Mol. Spectrosc.* **168**, 350 (1994).
- ¹⁴W. J. Balfour, J. Cao, C. X. W. Qian, and S. J. Rixon, *J. Mol. Spectrosc.* **183**, 113 (1997).
- ¹⁵A. J. Marr, M. E. Flores, and T. C. Steimle, *J. Chem. Phys.* **104**, 8183 (1996).
- ¹⁶R. S. Ram and P. F. Bernath, *J. Mol. Spectrosc.* **193**, 363 (1999).
- ¹⁷E. J. Friedman-Hill and R. W. Field, *J. Chem. Phys.* **100**, 6141 (1994).
- ¹⁸K. Y. Jung, T. C. Steimle, D. Dai, and K. Balasubramanian, *J. Chem. Phys.* **102**, 643 (1995).
- ¹⁹W. J. Balfour and R. S. Ram, *J. Mol. Spectrosc.* **105**, 360 (1984).
- ²⁰K. Jansson, R. Scullman, and B. Yttermo, *Chem. Phys. Lett.* **4**, 188 (1969).
- ²¹K. Jansson and R. Scullman, *J. Mol. Spectrosc.* **36**, 248 (1970).
- ²²H. Tan, M. Liao, and K. Balasubramanian, *Chem. Phys. Lett.* **280**, 219 (1997).
- ²³B. A. Palmer and R. Engleman, *Atlas of the Thorium Spectrum* (Los Alamos National Laboratory, Los Alamos, 1983).
- ²⁴H.-J. Werner and P. J. Knowles, *J. Chem. Phys.* **82**, 5053 (1985); P. J. Knowles and H.-J. Werner, *Chem. Phys. Lett.* **115**, 259 (1985).
- ²⁵D. Andrea, U. Häussermann, M. Dolg, H. Stoll, and H. Preuss, *Theor. Chim. Acta* **77**, 123 (1990).
- ²⁶A. Bergner, M. Dolge, W. Kuechle, H. Stoll, and H. Preuss, *Mol. Phys.* **80**, 1431 (1993).
- ²⁷R. S. Ram, J. Liévin, and P. F. Bernath, *J. Chem. Phys.* **109**, 6329 (1998).
- ²⁸R. S. Ram, J. Liévin, and P. F. Bernath, *J. Mol. Spectrosc.* (in press).
- ²⁹H.-J. Werner and P. J. Knowles, *J. Chem. Phys.* **89**, 5803 (1988); P. J. Knowles and H.-J. Werner, *Chem. Phys. Lett.* **145**, 514 (1988).
- ³⁰S. R. Langhoff and E. R. Davidson, *Int. J. Quantum Chem.* **8**, 62 (1974).
- ³¹MOLPRO (version 96.4) is a package of *ab initio* programs written by H.-J. Werner and P. J. Knowles, with contributions of J. Almlöf, R. D. Amos, M. J. O. Deegan, S. T. Elbert, C. Hampel, W. Meyer, K. Peterson, R. Pitzer, A. J. Stone, P. R. Taylor, and R. Lindh.
- ³²See AIP Document No. EPAPS: EJCPA6-111-009932, for two pages of data tables. EPAPS document files may be retrieved free of charge from AIP's FTP server (<http://www.aip.org/pubserv/paps.html>) or from <ftp.aip.org> in the directory /epaps/. For further information, e-mail: paps@aip.org or Fax: 516-576-2223.
- ³³R. Scullman and B. Yttermo, *Ark. Fys.* **33**, 231 (1966).
- ³⁴O. Appelblad, R. F. Barrow, and R. Scullman, *Proc. R. Soc. London* **91**, 261 (1967).
- ³⁵O. Appelblad, C. Nilsson, and R. F. Barrow, *Phys. Scr.* **7**, 65 (1973).
- ³⁶T. S. Steimle, K. Y. Jung, and B.-Z. Li, *J. Chem. Phys.* **102**, 5937 (1995).
- ³⁷B. Kaving and R. Scullman, *J. Mol. Spectrosc.* **32**, 475 (1969).